



## Effect of operational key parameters on photocatalytic degradation of phenol using nano nickel oxide synthesized by sol–gel method

Khizar Hayat<sup>a</sup>, M.A. Gondal<sup>b,\*</sup>, Mazen M. Khaled<sup>a</sup>, Shakeel Ahmed<sup>c</sup>

<sup>a</sup> Chemistry Department, King Fahd University of Petroleum & Minerals, Dhahran 31261, Saudi Arabia

<sup>b</sup> Laser Research Group, Physics Department and Center of Excellence in Nano Technology (CENT), King Fahd University of Petroleum & Minerals, Box 372, Dhahran 31261, Saudi Arabia

<sup>c</sup> Center for Refining and Petrochemical, Research Institute, King Fahd University of Petroleum & Minerals, Dhahran 31261, Saudi Arabia

### ARTICLE INFO

#### Article history:

Received 24 August 2010

Received in revised form

14 December 2010

Accepted 16 December 2010

Available online 24 December 2010

#### Keywords:

Nano nickel oxide

Heterogeneous photocatalysis

Phenol

Waste water treatment

Nanoparticles

### ABSTRACT

Photocatalytic oxidation of phenol was studied using nickel oxide (NiO) nanoparticles synthesized by sol–gel method. The morphology of synthesized catalyst was studied by using field emission scanning electron microscopy (FESEM), energy dispersive X-ray spectroscopy (EDX) and high resolution transmission electron microscopy (HRTEM) and X-ray diffraction (XRD). The average particle size was 6.5 nm as estimated by Scherrer formula and was confirmed by HRTEM and FESEM analysis. The photocatalytic activity of NiO was evaluated by degradation of phenol under irradiation of unique source like UV laser. The influence of various key parameters such as amount of photocatalyst, initial solution pH and the initial concentration of phenol was investigated. The operational parameters show the expected influence regarding the efficiency of the photocatalytic degradation process. The photocatalytic degradation efficiency of NiO was found to decrease with the increase in the initial solution pH. The degradation of the phenol followed a pseudo first-order rate kinetics with  $k=5.7 \times 10^{-2} \text{ min}^{-1}$ .

© 2010 Elsevier B.V. All rights reserved.

### 1. Introduction

Nanomaterials have recently attracted extensive interest for their unique properties in various fields as compared to their bulk counterparts [1–6]. Semiconductor metal oxide nanoparticles have been studied due to their novel optical, electronic, magnetic, thermal and mechanical properties and potential application in catalyst, gas sensors and photo–electronic devices [7–11]. More research has been focused on the types and modification of the catalyst, the photocatalytic principles, the factors influencing photocatalytic rate and the reaction kinetics [12–17]. Development of new photocatalysts for waste water treatment is of current interest [18]. These days, much attention has been focused to synthesize high-quality and ultra-fine powders with the required characteristics in terms of their size, morphology and microstructure. There are different methods reported for the synthesis of NiO nanoparticles, such as hydrothermal synthesis, carbonyl, and pulsed laser ablation, microemulsion, precipitation–calcination and sol–gel methods [19–23]. Compared with the conventional methods, sol–gel has many advantages.

Nanopowders could be prepared with narrow size distribution, higher purity, well dispersed and spherical shape by this method. Moreover, the physical and chemical properties of the nanopowders might be easily controlled by varying the processing parameters and no need of expensive agents or special equipment.

The uses of toxic compounds are creating a multiple environmental problems. There is an urgent demand to develop a method for solving these problems. Among these, removal of phenol and chlorinated phenols became more essential because of their high toxicity, extensive use and their weak retention in soil sediments. Sources of phenol include waste solutions in various industries, such as petroleum refining and plastics.

Traditional wastewater treatment techniques include activated carbon adsorption, chemical oxidation and biological digestion, in which the photoassisted catalytic decomposition of organic pollutants in water and wastewater employing semiconductors as photocatalysts has been a promising technique during the past two decades [24–29].

The photocatalytic process starts with the irradiation of a semiconductor material by light with sufficient energy to excite the electrons from the valence to the conduction band generating extremely reactive electron/hole ( $e^-/h^+$ ) pairs which migrate to the surface of the semiconductor where they can react with

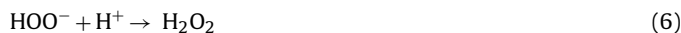
\* Corresponding author. Tel.: +966 38602351; fax: +966 38602293.

E-mail address: [magondal@kfupm.edu.sa](mailto:magondal@kfupm.edu.sa) (M.A. Gondal).

adsorbed species.



The hydroperoxyl radical formed in (4) also has scavenging property as  $\text{O}_2$  thus doubly prolonging the lifetime of photohole:



The ability of the photocatalytic technique to completely degrade organics into water and  $\text{CO}_2$ , without generating any harmful byproducts, has popularized its role as a wastewater purifier [30]. In the present work, a novel laser-based photocatalytic process has been tested for the degradation of phenol using NiO. In case of laser, there is high absorption of photons at a particular laser emission wavelength by photocatalysts as compared with broad spectral sources like lamps where most of the emission wavelengths lie outside the band gap energy of the catalyst. In addition, the drawback associated with the photo-degradation process with conventional setups using lamps is the longer irradiation time (hours or days) and thermal stability of UV lamp over longer periods of time [31–33]. Our purpose of use of laser as source of excitation in this study is to optimize the photo-degradation process and to identify the key parameters for optimization process and once these parameters are optimized, laser could be replaced with solar radiation for pilot plant studies.

The band gap of nano NiO is in the range of 3.6–3.8 eV as reported in the literature [34,35] therefore 266 nm wavelength (UVC) was applied for the optimization of the process for the first time in this work to enhance the degradation process.  $\text{TiO}_2$  is well studied catalyst for photocatalytic applications [36]. However, for improvement of efficiency and to enhance the reaction rate, work on other catalysts like ZnO, NiO,  $\text{Fe}_2\text{O}_3$  and  $\text{MnO}_2$  is being investigated worldwide [37]. Under our experimental conditions, nano-NiO catalysts demonstrated better photocatalytic efficiency for degradation of phenol at 266 nm as compared with  $\text{TiO}_2$ . The reason could be the suitability of band gap for NiO at 266 nm and the nano structured nature of the self synthesized NiO applied in this work.

In this paper, NiO nanoparticles were synthesized by sol-gel method and characterized by the use of X-ray diffraction (XRD), field emission electron microscopy (FESEM) and high resolution transmission electron microscopy (TEM). The photocatalytic activity of nano NiO was investigated for the oxidation of phenol in aqueous solution. The effect of key operational parameters on phenol degradation process such as amount of catalyst, initial pH and phenol concentration was also studied.

## 2. Experimental

### 2.1. Materials

Chemicals such as  $\text{Ni}(\text{NO}_3)_2 \cdot 6\text{H}_2\text{O}$  and citric acid monohydrate used in the preparation of nano-NiO particles, were of analytical grade and were used without further purification. Deionized water was used throughout the study. Phenol used in this study was purchased from Fluka. Methanol of HPLC grade was used as solvent.

### 2.2. Catalyst synthesis and its characterization

Nickel oxide nanoparticles were prepared using the sol-gel process. Appropriate amount of  $\text{Ni}(\text{NO}_3)_2 \cdot 6\text{H}_2\text{O}$  and citric acid

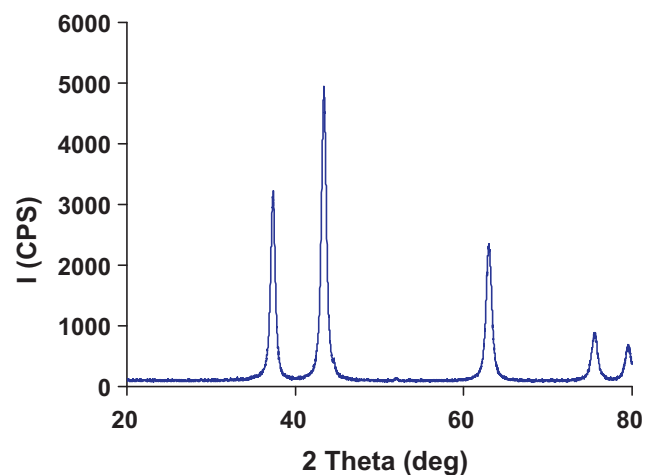


Fig. 1. X-ray diffractogram of nano NiO calcined at 500 °C.

monohydrate were accurately weighed and dissolved in deionized water. Subsequently, the mixed solution was heated at a temperature of 65 °C with continuous stirring for three days. The green gel so obtained was dried at 100 °C for 24 h. The precursors were heated in a programmable furnace at the rate of 1 °C/min to achieve the temperature of 500 °C and allowed to stay for 6 h at this temperature.

The crystalline structure of the product was characterized by a rotating-target X-ray diffractometer (Japan Rigaku D/Max-2400) equipped with a monochromatic high-intensity  $\text{Cu K}\alpha$  radiation ( $=1.5418 \text{ \AA}$ , 40 kV, 100 mA). The average crystalline size of the NiO nanoparticles was estimated from the full width half maximum (FWHM) and the peak position of an XRD line broadened according to the Scherrer formula [38]:

$$d = \frac{0.9\lambda}{B \cos \theta} \quad (7)$$

where  $d$  is the average crystallite size,  $\lambda$  is the wavelength of the X-ray (0.15418 nm),  $B$  is the full width at half maximum (FWHM, radian) and  $\theta$  is the Bragg angle (degree). The value of FWHM was obtained by performing profile fitting using an XRD pattern processing software. The mean particle size of the as-synthesized products is calculated according to this at about 6.5 nm and further confirmed with the help of SEM and TEM results.

The peaks positions appear at  $2\theta = 37.20^\circ$ ,  $43.20^\circ$ ,  $62.87^\circ$ ,  $75.20^\circ$  and  $79.38^\circ$  as depicted in Fig. 1 and can be indexed as (1 1 1), (2 0 0), (2 2 0), (3 1 1), and (2 2 2) crystal planes of the bulk NiO, respectively. All these diffraction peaks can be perfectly indexed to the face centered cubic (FCC) crystalline structure of NiO which is in accordance with that of the standard spectrum (JCPDS No. 04-0835). The XRD pattern shows that the samples are single-phase and no any other impurities distinct diffraction peak except the characteristic peaks of FCC phase NiO was detected.

Fig. 2(a) and (b) shows the FESEM image and EDX of NiO nanoparticles. It is evident from Fig. 2(a) that the NiO nanoparticles had spherical shapes and were well dispersed with smooth surface and uniform size. Fig. 3 shows a HRTEM micrograph of the NiO nanoparticles. The results of FESEM and HRTEM observations further confirmed and verified the relevant results obtained by XRD.

### 2.3. Photocatalytic degradation of phenol

Photocatalytic activity of the synthesized photocatalyst was evaluated using aqueous solution of phenol under ultraviolet laser (266 nm) irradiation. The experiments were carried out in a locally

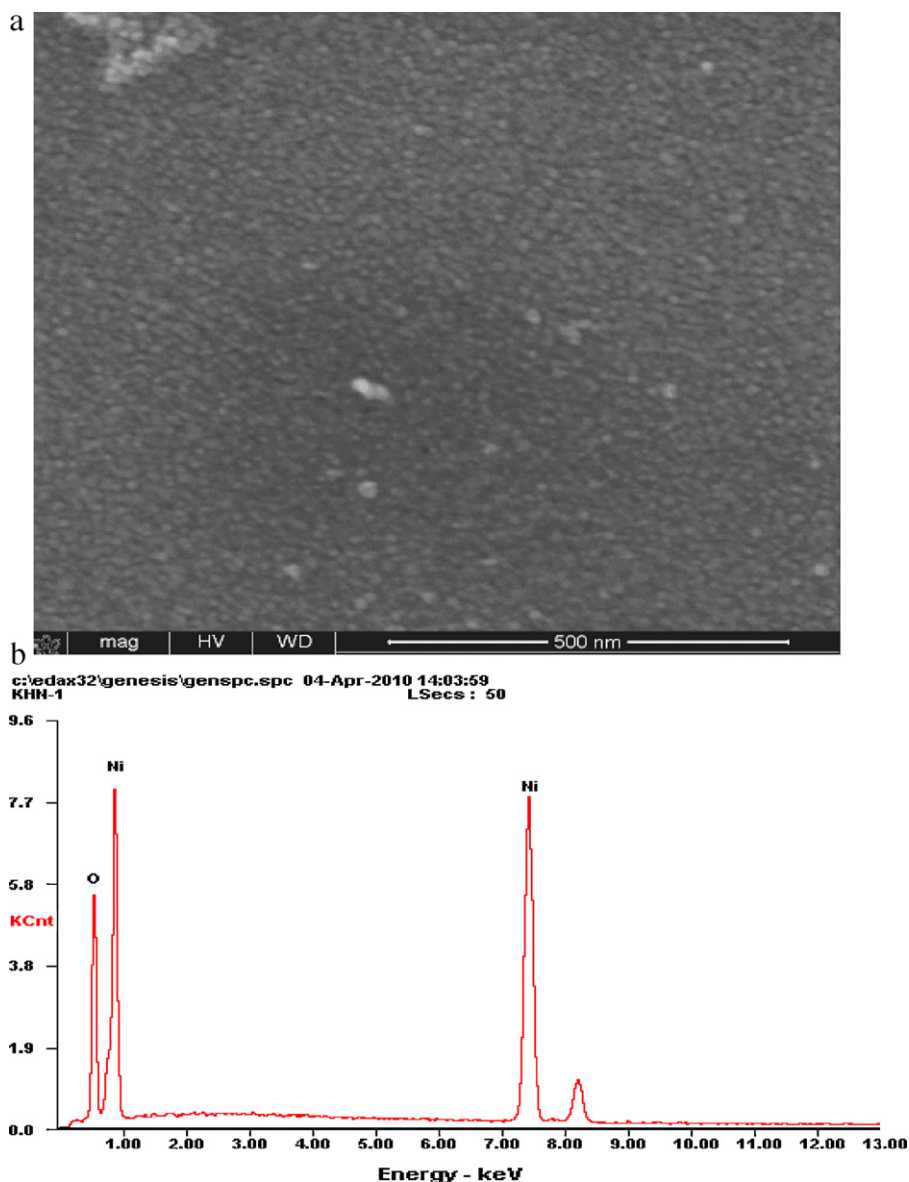


Fig. 2. (a) Field emission scanning electron micrograph of nano NiO. (b) Energy dispersive X-ray spectroscopy of nano NiO.

designed photocatalytic reactor with quartz window for illumination of UV laser irradiation. The stock solution of phenol containing  $100 \text{ mg L}^{-1}$  was prepared in deionized water. The photoreactor was loaded with 100 mL of aqueous suspension of nano NiO in phenol. The aqueous suspension was magnetically stirred in the dark for 15 min to ensure the establishment of adsorption equilibrium. Then, the suspension was irradiated with UV light at constant stirring speed and laser energy. Nd: YAG laser (Brilliant B Quantel,  $\lambda = 266 \text{ nm}$ , pulse duration = 6 ns) was used to irradiate the solution. After regular intervals, 5.0 mL of the sample was withdrawn from the reactor and filtered using nano syringe filters. High performance liquid chromatograph (Waters 2996 Photodiode Array Detector, Waters 1525 Binary HPLC pump and Waters 717 plus Autosampler) was used to analyse the laser irradiated samples. The stationary phase consisted in a Purospher Star RP-18 endcapped column ( $250 \text{ mm} \times 4.6 \text{ mm}$ ,  $5 \mu\text{m}$  particles) working at room temperature. A mixture of water and methanol with a gradient concentration was used as the mobile phase at a flow rate of  $1.0 \text{ mL min}^{-1}$ . The removal of phenol after time  $t$  was calculated by peak area method. To study the effect of pH on photodegradation rate, the initial pH

of the suspension was adjusted by the addition of either NaOH or  $\text{HNO}_3$  solutions.

### 3. Results and discussion

#### 3.1. Effect of laser UV irradiation and photocatalyst containing phenol using nano NiO

Photocatalytic degradation of phenol was investigated without NiO catalyst as well as in the absence of laser UV light. Only nano NiO catalyst without UV laser irradiation could not catalyze the degradation of the phenol. It was observed that phenol degradation was not significant in the absence of laser or nano NiO. The results indicate that both the catalyst and light are essential for efficient phenol degradation. The photodegradation of phenol in aqueous solution as a function of laser irradiation time in the presence of nano-structured NiO is shown in Fig. 4.

The rate constant obtained from the plot shown in Fig. 5 was  $5.7 \times 10^{-2} \text{ min}^{-1}$ . The percentage degradation of phenol was cal-

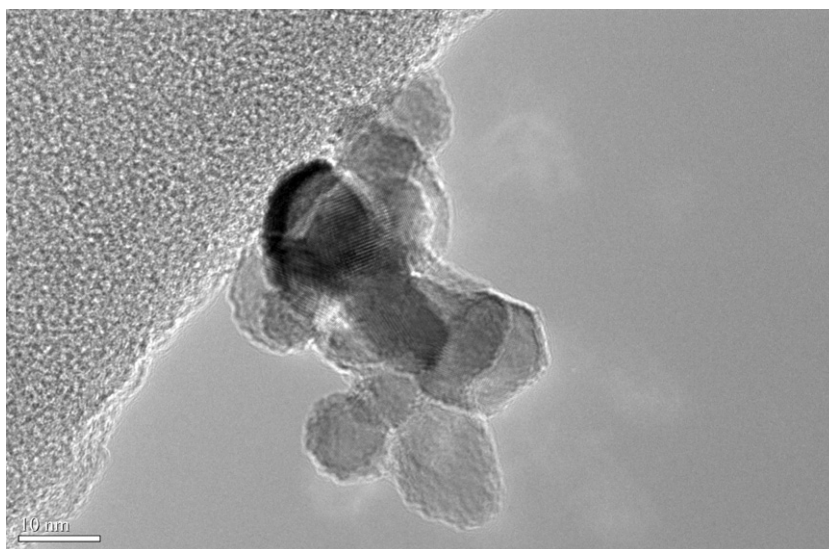


Fig. 3. High resolution transmission electron micrograph of nano NiO.

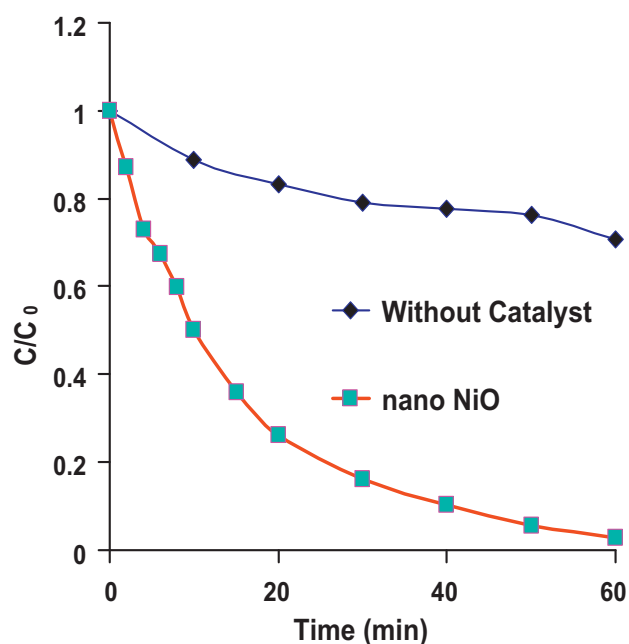


Fig. 4. A plot showing the degradation of phenol as a function of laser exposure time for an aqueous solution of phenol in presence of NiO. Experimental conditions: phenol concentration = 1.064 mM, V = 100 mL, NiO = 1.0 g L<sup>-1</sup>, and laser exposure time = 60 min.

culated using the following relation:

$$\text{Phenol degradation (\%)} = \frac{1 - C_t}{C_0} \times 100 \quad (8)$$

where  $C_0$  = initial concentration of phenol and  $C_t$  = concentration of phenol at any time 't'.

The results demonstrate that almost 97% of phenol was degraded within 60 min using laser irradiation by nano NiO catalyst. The results obtained in this study demonstrate that the percentage of phenol degradation increases with the increase in laser irradiation exposure time. This increase in phenol degradation might be due to increase in the amount of produced OH<sup>•</sup> radicals with time.

### 3.2. Effect of catalyst weight on photocatalytic degradation of phenol using nano NiO

The optimum weight of catalyst is an important parameter to be investigated to avoid ineffective excess of catalyst and to ensure the total absorption of efficient photons. For this study, the weight of nano NiO in the suspension was varied from 1.0 to 6.0 g L<sup>-1</sup>. An increase in the catalyst loading up to an amount of 6.0 g L<sup>-1</sup> resulted in a decrease in the rate constant as depicted in Fig. 6 which can be attributed to a screening effect due to the redundant dispersion of UV radiation caused by the ample amount of suspended photocatalyst. In addition, particles tend to agglomerate, making a significant fraction of the catalyst to be inaccessible to either adsorbing the molecules or absorbing the laser radiations, with consequent decrease in the active sites available to the catalytic reaction [39,40]. The results presented in Table 1 indicate

Table 1  
Effect of key parameters on photo-degradation rate of phenol using nano-NiO.

Parameters		Rate constant $k$ (min <sup>-1</sup> )	$R^2$	Photodegradation rate ( $\mu\text{M min}^{-1}$ )
Catalyst loading (g L <sup>-1</sup> )	1.0	0.0570	0.9641	60.65
	2.0	0.0540	0.9809	57.46
	3.0	0.0481	0.9732	51.18
	4.0	0.0433	0.9643	46.07
	6.0	0.0321	0.8879	34.15
Initial solution pH	5.0	0.0663	0.9885	70.54
	6.5	0.0582	0.9727	61.93
	9.0	0.0254	0.9475	27.03
	11.0	0.0115	0.9315	12.24

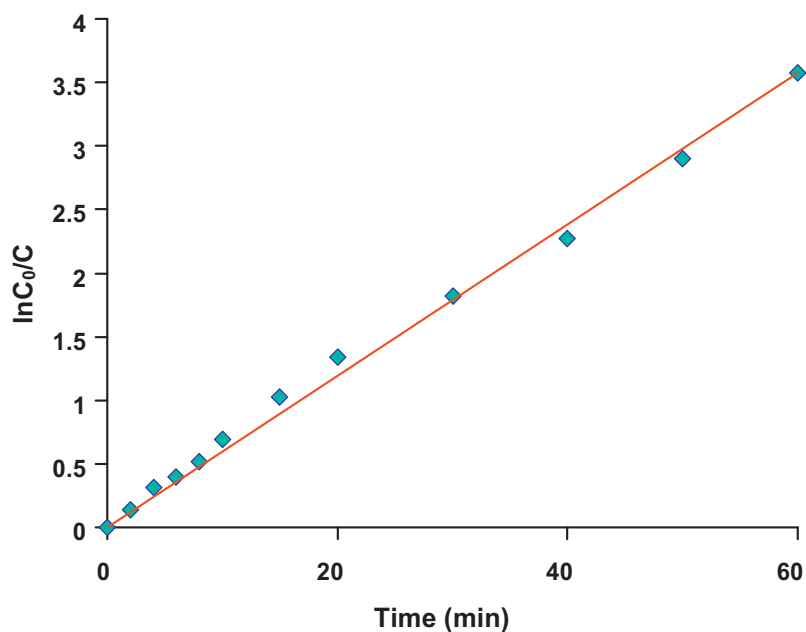


Fig. 5. A plot of  $\ln C_0/C$  as a function of laser irradiation time for an aqueous solution of phenol in presence of NiO.

that the photodegradation rate decreases as the amount of catalyst increases from 1.0 to 6.0 gL<sup>-1</sup>. Following these observations, it was decided to keep the amount of nano NiO at the optimum value of 1.0 gL<sup>-1</sup> in subsequent photocatalytic degradation experiments.

### 3.3. Effect of pH on photocatalytic degradation of phenol using nano NiO

The pH of the suspension was varied in the range (5.0–11.0) to study its effect on the photocatalytic degradation of phenol. The plot of pH versus  $\ln C_0/C$  is depicted in Fig. 7. It is evident from the results that the photocatalytic degradation rate was increased when pH was decreased from natural to pH=5. It is clear from

the results presented in Table 1 that the photoefficiency of the process decreases and phenol removal becomes slow with a  $k$  of  $1.15 \times 10^{-3} \text{ min}^{-1}$  at pH 11. Similar behavior of photocatalysts was also reported by some researchers during their studies [41–43].

Nano NiO shows amphoteric behavior in aqueous media. Electric charge properties of both, catalyst and substrate, are found to play an important role on adsorption process. The point of zero charge (pzc) of nano NiO, i.e. the point at which the surface charge density is zero, was found to be of 10.5 [44]. At pH higher than  $\text{pH}_{\text{pzc}}$  nano NiO surface is negatively charged and  $\text{NiO}^{\bullet-}$  appears to be the predominant form of NiO. For lower pH values, nano NiO surface is in the protonated form ( $\text{Ni OH}^{2+}$ ). Phenol shows a  $\text{pK}_a$  of 9.9 (at 25 °C) under aqueous media. If  $\text{pH} < \text{pK}_a$ , phenol

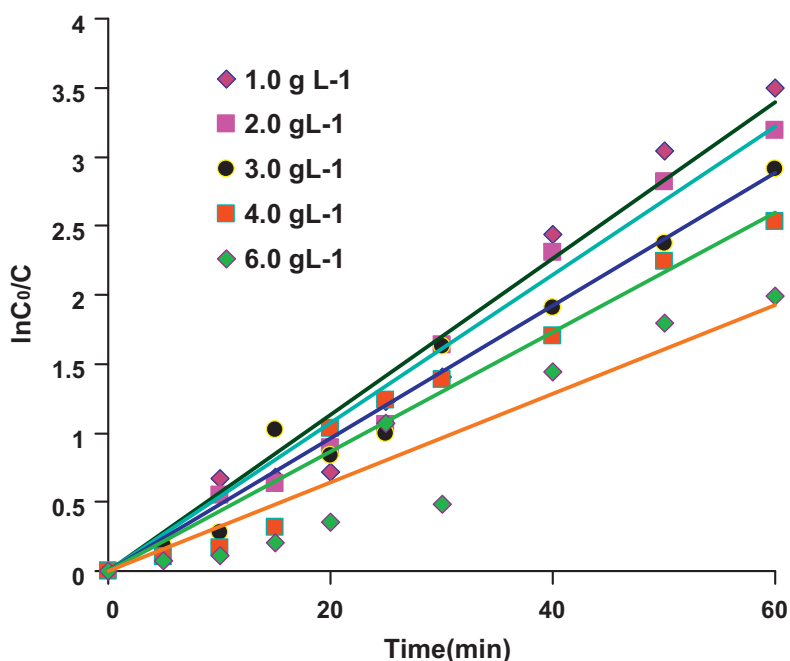


Fig. 6. The change of rate constant as a function of catalyst loading for photocatalytic degradation of phenol using NiO.

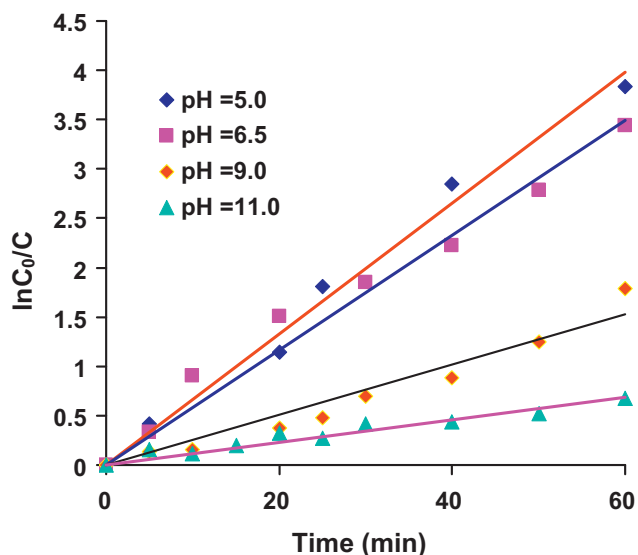


Fig. 7. Effect of initial pH on photodegradation of aqueous solution of phenol in presence of NiO.

is in the molecular form ( $C_6H_5OH$ ) and at  $pH > pK_a$  the molecule undergoes deprotonation becoming negatively charged ( $C_6H_5O^-$ ). Under these conditions, both catalyst and substrate are negatively charged, developing repulsive forces between them. Consequently, the phenol adsorption is decreased, which decreases its degradation.

#### 3.4. Effect of concentration on photocatalytic degradation of phenol using nano NiO

The effect of initial phenol concentration was investigated varying the concentration from 0.532 mM to 2.66 mM which is depicted in Fig. 8. The photo degradation rates are presented in Table 2. The degradation rate for decomposition of the phenol under investigation was found to increase with the increase in substrate concentration up to a certain level and reaches to saturation limit which is in agreement with a number of studies reported earlier [45]. This saturation trend of degradation rate could be due to the scavenging of the majority of photogenerated OH radicals by phenol at its higher concentration.

The photocatalysed degradation of phenol in solution is initiated by the photoexcitation of the semiconductor, followed by the formation of electron–hole pair on the surface of catalyst. Highly oxidative valence band holes and various oxygen-containing radical species (e.g.,  $\cdot OH$ ,  $O_2^{\cdot -}$ ,  $HO_2^{\cdot}$ ) are produced [46]. Among these species, holes and  $\cdot OH$  radicals play the most important roles in the photodegradation of organic pollutants. The high oxidative potential of the hole ( $h_{VB}^+$ ) in the catalyst permits the direct oxidation of phenol to reactive intermediates. The overall quantum efficiency depends from the competition between charge–carrier recombination, trapping, and interfacial charge transfer.

Table 2  
Effect of substrate concentration on rate constant of phenol degradation using nano-NiO.

S. no.	Phenol conc. (mM)	$(k_{app})/min^{-1}$	Photodegradation rate ( $10^{-5} M min^{-1}$ )	$R^2$	$1/k_{app}$
1	0.532	0.0876	4.66	0.8833	11.42
2	1.064	0.0613	6.52	0.986	16.31
3	1.596	0.0430	6.86	0.9977	23.25
4	2.128	0.0317	6.74	0.9415	31.55
5	2.66	0.0246	6.54	0.9691	40.65

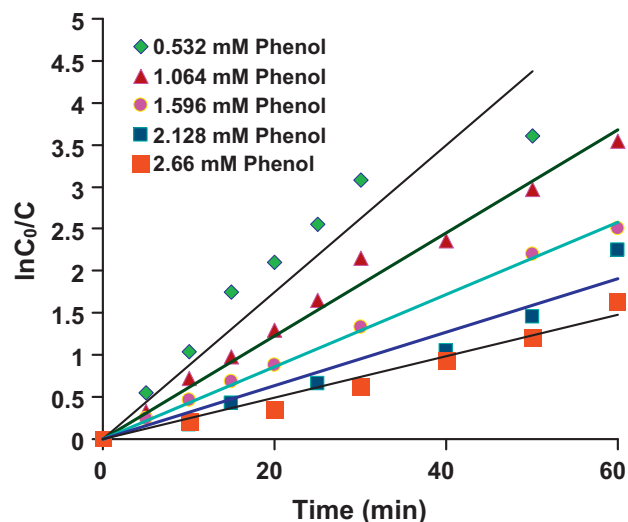


Fig. 8. The diagram showing the effect of initial dye concentration on photocatalytic degradation rate of phenol by nano NiO.

#### 3.5. Kinetics of photocatalytic degradation phenol

The kinetic of photocatalytic degradation of phenol obeys pseudo first order behavior and can be expressed as equations. i.e.:

$$\text{rate} = \frac{-dC}{dt} = \frac{kKC}{1 + KC} = k_{app}C \quad (9)$$

$$\frac{1}{k_{app}} = \frac{1}{k_c K} + \frac{C_0}{k_c} \quad (10)$$

where  $C_0$  = initial concentration of phenol;  $C$  = concentration of phenol at any time ' $t$ ';  $k$ ,  $k_{app}$  denote rate constant, and the apparent pseudo-first order rate constant, respectively.  $K$  and  $k_c$  are phenomenological constants that depend on some operational factors including the radiation intensity. The reaction mechanism considered for heterogeneous photocatalyzed reactions consist of two main steps: fast adsorption of the reactants on the catalyst surface and a slow step of reaction in the adsorbed phase of the organic compound and a photogenerated hydroxyl radical. The results reported in the literature [47,48] demonstrate that  $k_c$  and  $K$  are light intensity-dependent.

A plot of  $1/k_{app}$  versus initial dye concentration is presented in Fig. 9. In photo-induced reactions, the number of active catalyst sites is less than the total surface adsorption sites. Both  $k_c$  and  $K$  depend on the intensity of absorbed light. Results showed that  $k_c$  is proportional to the incident photon flux while  $K$  decreased for higher light intensity [49–52]. Experimental data reported in Table 2 demonstrate that photocatalytic oxidation of phenol follows a pseudo-first order kinetic model. As photon flow increases, the number of photogenerated  $HO^{\cdot}$  radicals rise up, accelerating the oxidation of the substrate molecules. Simultaneously, the increase of surface active species such as electrons, holes and  $HO^{\cdot}$  radicals lead to a decrease in the available sites for adsorption of the primary molecule and therefore a decrease in  $K$ .

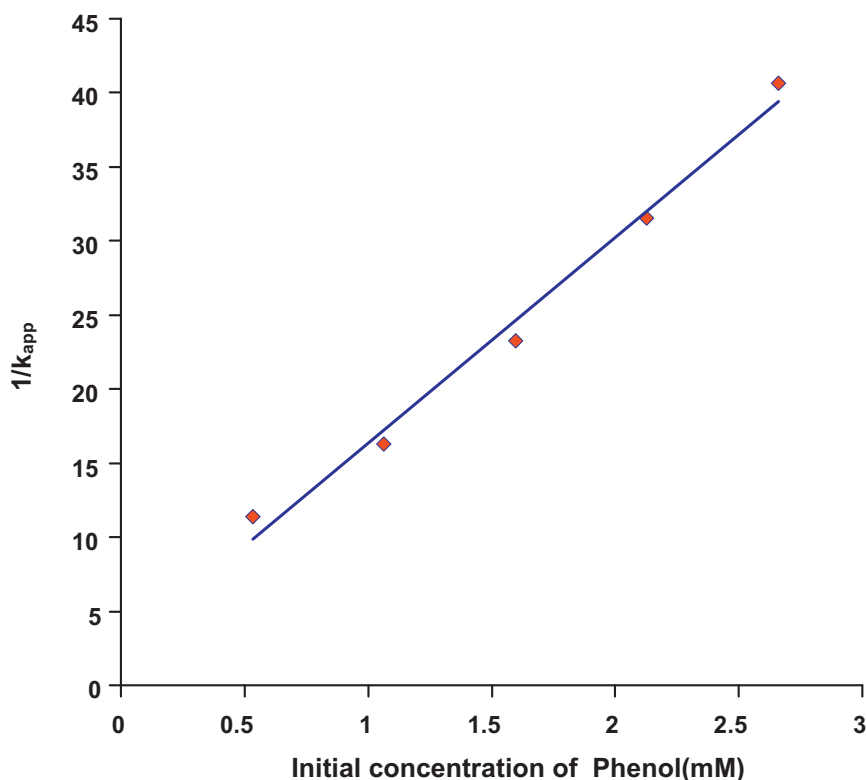


Fig. 9. A plot of  $1/k_{app}$  against initial phenol concentration.

#### 4. Conclusions

Cubic NiO nanoparticles with spherical shape, higher purity, well-dispersed and narrow size distribution ranging from 6 to 10 nm were successfully synthesized by sol-gel method and different approaches such as XRD, FESEM and HRTEM were used to characterize the nano-NiO particles. The average particle size obtained from the XRD was confirmed by HRTEM analysis. Photocatalytic degradation of phenol (97%) using nano NiO and UV laser irradiation was achieved within short span of time as compared with conventional setups like lamps. The degradation rate was increased significantly by increasing the initial pH of the solution while it decreases with increasing substrate concentration. The results obtained obey pseudo-first order rate kinetics.

#### Acknowledgements

The support by King Fahd University of Petroleum and Minerals and KACST through projects 08-NAN93-4 is gratefully acknowledged. One of the authors (Khizar Hayat) is thankful to KFUPM for graduate assistantship.

#### References

- [1] H. Gleiter, Prog. Mater. Sci. 33 (4) (1990) 223.
- [2] G.Z. Wang, L.D. Zhang, J.M. Mou, Acta Phys. Chim. 13 (5) (1997) 445.
- [3] Y. Xie, J. Huang, B. Li, Y. Liu, Y. Qian, Adv. Mater. 12 (2000) 1523.
- [4] S. Yu, M. Yoshimura, Adv. Mater. 14 (2002) 296.
- [5] T. Mokari, U. Banin, Chem. Mater. 15 (2003) 3955.
- [6] W. Wang, I. Germanenko, Chem. Mater. 14 (2002) 3028.
- [7] W. Lee, M.C. Jeong, J.M. Myoung, Acta Mater. 52 (2004) 3949.
- [8] C.L. Xu, D.H. Qin, H. Li, T. Xu, H.L. Li, Mater. Lett. 58 (2004) 3976.
- [9] W.I. Park, Y.H. Jun, S.W. Jung, G.C. Yi, Appl. Phys. Lett. 82 (2003) 964.
- [10] F. Takehia, O. Satoshi, O. Hajime, et al., J. Power Sources 86 (2001) 340.
- [11] J.L. Katz, P.F. Miquel, Nanostruct. Mater. 4 (5) (1994) 551.
- [12] St. Christoskova, M. Stoyanova, Water Res. 35 (2001) 2073.
- [13] K.H. Wong, S. Tao, R. Dawson, P.K. Wong, Hazard. Mater. B 109 (2004) 149.
- [14] K.-H. Wang, Y.-H. Hsieh, M.Y. Chou, C.-Y. Chang, Appl. Catal. B: Environ. 21 (1999) 1.
- [15] A. Cybulski, J. Trawczyński, Appl. Catal. B: Environ. 47 (2004) 1.
- [16] H. Chun, W. Yizhong, T. Hong Xiao, Environ. Sci. 18 (1997) 1.
- [17] J.C. Yu, W. Ho, J. Yu, S.K. Hark, K. Lu, Langmuir 19 (2003) 3889.
- [18] W. Han, W. Zhu, P. Zhang, Y. Zhang, L. Li, Catal. Today 90 (2004) 319.
- [19] I. Hotovy, J. Huran, L. Spiess, et al., Sens. Actuators B 57 (1999) 147.
- [20] H. Bi, S.D. Li, Y.C. Zhang, J. Magn. Magn. Mater. 277 (3) (2004) 363.
- [21] Y.D. Li, C.W. Li, X.F. Duan, et al., J. China Univ. Sci. Technol. 27 (3) (1997) 346.
- [22] W.Z. Wang, Y.K. Liu, C.K. Xu, et al., Chem. Phys. Lett. 362 (1–2) (2002) 119.
- [23] Z.Q. Wei, T.D. Xia, L.F. Bai, et al., Mater. Lett. 60 (3) (2006) 766.
- [24] D.F. Ollis, C.S. Turchi, Environ. Prog. (1990) 229.
- [25] M.R. Hoffmann, S.T. Martin, W. Choi, D.W. Bahnemann, Chem. Rev. 95 (1995) 69.
- [26] A. Mills, S.L. Hunte, J. Photochem. Photobiol. A 108 (1997) 1.
- [27] J.M. Hermann, Catal. Today 53 (1999) 115.
- [28] M.I. Litter, Appl. Catal. B: Environ. 23 (1999) 89.
- [29] A. Fujishima, T.N. Rao, D.A. Tryk, J. Photochem. Photobiol. C: Photochem. Rev. 1 (2000) 1.
- [30] H. Gerixhac, Electrochim. Acta 38 (1993) 39.
- [31] A. Orlov, D.A. Jefferson, N. Macleod, R.M. Lambert, Catal. Lett. 92 (2004) 41.
- [32] D. Hufschmidt, D. Bahnemann, J.J. Testa, C.A. Emilio, M.I. Litter, J. Photochem. Photobiol. A: Chem. 148 (2002) 223.
- [33] H. Iida, K. Yonezawa, M. Kosaka, A. Igarashi, Catal. Commun. 10 (2009) 627.
- [34] X. Wang, J. Song, L. Gao, J. Jin, H. Zheng, Z. Zhang, Nanotechnology 16 (2005) 37.
- [35] T. Okazawa, M. Fujiwara, T. Nishimura, T. Akita, M. Kohyama, Y. Kido, Surf. Sci. 600 (2006) 1331.
- [36] H. Fujii, M. Ohtaki, K. Eguchi, J. Am. Chem. Soc. 120 (1998) 6832.
- [37] H.M. Kang, X.H. Kang, Trans. Tianjin Univ. 2 (2) (1996) 44.
- [38] X.M. Liu, X.G. Zhang, S.Y. Fu, Mater. Res. Bull. 41 (3) (2006) 620.
- [39] W. Baran, A. Makowski, W. Wardas, Chemosphere 59 (2005) 853.
- [40] E. Bizani, K. Fytianos, I. Poullos, V. Tsiroidis, J. Hazard. Mater. 136 (2006) 85.
- [41] H. Lachheb, E. Puzenat, A. Houas, M. Ksibi, E. Elaoui, G. Guillard, J.M. Hermann, Appl. Catal. B: Environ. 39 (2002) 75.
- [42] M. Styliidi, D.I. Kondarides, X.E. Verykios, Appl. Catal. B: Environ. 40 (2003) 271.
- [43] I.K. Konstantinou, T.A. Albanis, Appl. Catal. B: Environ. 49 (2004) 1.
- [44] J.A. Lewis, J. Am. Ceram. Soc. 83 (2000) 2341.
- [45] J.M. Herrmann, Top. Catal. 34 (2005) 49.

- [46] A. Saber, M.G. Rasul, N.M. Wayde, R. Brown, M.A. Hashib, *Desalination* 261 (2010) 3.
- [47] A. Mills, J. Wang, D.F. Ollis, *J. Phys. Chem. B* 110 (2006) 14386.
- [48] D.F. Ollis, *Top. Catal.* 35 (2005) 217.
- [49] S. Brosillon, L. Lhomme, C. Vallet, A. Bouzaza, D. Wolbert, *Appl. Catal. B: Environ.* 78 (2008) 232.
- [50] G. Palmisano, M. Addamo, V. Augugliaro, T. Caronna, A.D. Paola, E.G. López, V. Lodo, G. Marci, L. Palmisano, M. Schiavello, *Catal. Today* 122 (2007) 118.
- [51] C. Minero, *Catal. Today* 54 (1999) 205.
- [52] D. Vione, C. Minero, V. Maurino, M.E. Carloti, T. Picatonotto, E. Pelizzetti, *Appl. Catal. B* 58 (2005) 79.